Implications of large elastic thicknesses for the composition and current thermal state of Mars

M. Grott, D. Breuer

Accepted Manuscript

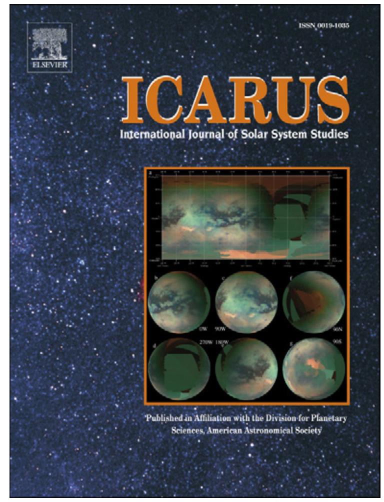

Implications of large elastic thicknesses for the composition and current thermal state of Mars

M. Grott, D. Breuer

PII: S0019-1035(09)00044-X
DOI: 10.1016/j.icarus.2009.01.020
Reference: YICAR 8904

To appear in: *Icarus*

Received date: 22 July 2008
Revised date: 15 January 2009
Accepted date: 23 January 2009

Please cite this article as: M. Grott, D. Breuer, Implications of large elastic thicknesses for the composition and current thermal state of Mars, *Icarus* (2009), doi: 10.1016/j.icarus.2009.01.020

Implications of large elastic thicknesses for the composition and current thermal state of Mars

M. Grott [a] D. Breuer [a]

[a] *Institute of Planetary Research, German Aerospace Center (DLR), Rutherfordstraße 2, 12489 Berlin, Germany*

Pages	41
Tables	0
Figures	6

Running Title: "Composition and current thermal state of Mars"

Corresponding Author:

Matthias Grott

German Aerospace Center (DLR)

Rutherfordstraße 2

12489 Berlin

Germany

email: matthias.grott@dlr.de

phone: +49-30-67055-419

Abstract

The Martian elastic lithosphere thickness T_e has recently been constrained by modeling the geodynamical response to loading at the Martian polar caps and T_e was found to exceed 300 km at the north pole today. Geological evidence suggests that Mars has been volcanically active in the recent past and we have reinvestigated the Martian thermal evolution, identifying models which are consistent with $T_e > 300$ km and the observed recent magmatic activity. We find that although models satisfying both constraints can be constructed, special assumptions regarding the concentration and distribution of radioactive elements, the style of mantle convection and/or the mantle's volatile content need to be made. If a dry mantle rheology is assumed, strong plumes caused by, e.g., a strongly pressure dependent mantle viscosity or endothermic phase transitions near the core-mantle boundary are required to allow for decompression melting in the heads of mantle plumes. For a wet mantle, large mantle water contents of the order of 1000 ppm are required to allow for partial mantle melting. Also, for a moderate crustal enrichment of heat producing, elements the planet's bulk composition needs to be 25% and 50% sub-chondritic for dry and wet mantle rheologies, respectively. Even then, models resulting in a globally averaged elastic thicknesses of $T_e > 300$ km are difficult to reconcile with most elastic thickness estimates available for the Hesperian and Amazonian periods. It therefore seems likely that large elastic thicknesses in excess of 300 km are not representative for the bulk of the planet and that T_e possibly shows a large degree of spatial heterogeneity.

Key words: Mars; Mars Interior; Thermal Histories; Geophysics

1 Introduction

In the absence of direct measurements, the elastic lithosphere thickness T_e is one of the few clues we have to the thermal state a planet, enabling us to reconstruct its thermal history. The latter significantly influences tectonic, magmatic and geological processes present on the surface and Phillips et al. (2008) have recently studied the geodynamical response of the Martian lithosphere to loading by the northern polar cap to constrain the present day Martian elastic lithosphere thickness.

Using radar sounding data obtained by SHARAD, the shallow radar onboard the Mars Reconnaissance Orbiter, Phillips et al. (2008) found that the Martian lithosphere is extremely stiff and T_e is larger than 300 km at the north pole today. This is surprising as this value is almost twice as large as previously estimated from theoretical considerations (Grott and Breuer, 2008a). Also, the best fit elastic thickness derived from flexure studies of the south polar load yields $T_e = 140$ km, although any value greater than 102 km can fit the observations (Wieczorek, 2008).

Phillips et al. (2008) propose three solutions to explain these large elastic thicknesses: First, elastic thicknesses could be spatially heterogeneous, being small near the volcanic centers of Tharsis and Elysium and large in the polar regions. In this case, the estimated $T_e > 300$ km would not be representative for the bulk of the planet and the average elastic thickness would be somewhat smaller. Second, the Planum Boreum load could not be in dynamic equilibrium, i.e., the small amount of deflection could result from a transient state of the planetary interior. In this case, the current elastic thickness at the north pole could be smaller than 300 km. Finally, if $T_e > 300$ km is representative for the bulk of the planet, the planetary interior needs to be relatively cold and Phillips et al. (2008) propose that the bulk concentration of radiogenic elements in the Martian interior could be sub-chondritic.

Of these approaches, the last two appear to be problematic: First, as shown by Phillips et al. (2008), it is difficult to construct models with small elastic thicknesses that do not result in deflections well exceeding the observed value one Myr after loading. Second, geochemical analysis of the SNC meteorites implies essentially chondritic concentrations of radioactive elements (Wänke and Dreibus, 1994; Treiman et al., 1986; Lodders and Fegley, 1997). Furthermore, if the concentration of heat producing elements in the Martian interior is indeed reduced, the resulting low interior temperatures could possibly inhibit partial mantle melting and magmatism. However, geological evidence suggests that Mars has been volcanically active in the recent past [e.g., Neukum et al. (2004)].

This study will explore the implications of large elastic thicknesses and we will assume that $T_e > 300$ km is globally representative. We will reinvestigate the

Martian thermal evolution considering wet as well as dry mantle rheologies. Different compositional models in terms of the bulk content of heat producing elements will be investigated and models which are compatible with the large elastic thicknesses reported by Phillips et al. (2008) will be identified. Furthermore, the evolution of the elastic lithosphere thickness predicted by these models will be compared to the available elastic thickness estimates derived from gravity and topography data (McGovern et al., 2004; Belleguic et al., 2005; Hoogenboom and Smrekar, 2006; Wieczorek, 2008), forward modeling of thrust faults (Schultz and Watters, 2001; Grott et al., 2006), the analysis of rift flank uplift (Grott et al., 2005; Kronberg et al., 2007) and the new estimate by Phillips et al. (2008). Finally, we will address the question of whether these models are compatible with the production of partial melt in the Martian mantle today.

2 Model

2.1 Thermal evolution and elastic thickness

The thermal evolution of Mars is modelled solving the energy balance equations for the core, mantle and lithosphere, treating the mantle energy transport by parametrized convection models using scaling laws for stagnant lid convection (Grasset and Parmentier, 1998). The model is similar to that of Grott and Breuer (2008a) and we ignore crustal production. Instead, we assume that the bulk of the crust is primordial and although there is evidence for late crustal production even after 4 Gyr (Hartmann et al., 1999; Hartmann and Berman, 2000; Neukum et al., 2004; Grott, 2005), its volumetric contribution is probably minor on a global scale (Nimmo and Tanaka, 2005). Note that the latent heat of melting associated with crustal production can have a large influence on the total amount of melt produced during the evolution (Hauck and Phillips, 2002), but does not significantly affect the current thermal state of Mars as it is expected to change the mantle energy balance by less than one percent. Details of the model used here may be found in Grott and Breuer (2008a).

Thermal evolution models start from temperature profiles that vary adiabatically in the core and mantle and the core is assumed to be superheated with respect to the mantle by 300 K (Stevenson, 2001; Breuer and Spohn, 2003). Cooling of the planet is then controlled by mantle convection and the mantle viscosity determines the efficiency of the heat transport, the thickness of the thermal boundary layers and the temperatures in the Martian lithosphere.

Given the thermal structure of the lithosphere, the elastic lithosphere thicknesses T_e is calculated using the strength envelope formalism (McNutt et al., 1988) for the two-layer system consisting of crust and mantle. Given the rheologies for the crust and mantle the elastic thicknesses of the individual crustal and mantle layers $T_{e,c}$ and $T_{e,m}$ are calculated. As the numerical results will be compared to the elastic thickness derived from the non-flexed lithosphere at the north pole, zero bending moment is assumed for the calculation of $T_{e,c}$ and $T_{e,m}$.

The elastic thickness of the compound system consisting of the crust and mantle layers then depends on whether the individual layers are welded or separated by a layer of incompetent crust. If the layers are detached, T_e is given by

$$T_e = (T_{e,m}^3 + T_{e,c}^3)^{\frac{1}{3}} \tag{1}$$

where $T_{e,m}$ and $T_{e,c}$ are the thicknesses of the elastic portions of the mantle and crust, respectively (e.g., Burov and Diament (1995)). If, however, $T_{e,c}$ equals the crustal thickness and no layer of incompetent crust exists, T_e is simply given by the sum of the individual components which then act as a single plate and

$$T_e = T_{e,m} + T_{e,c} \tag{2}$$

Details of the this model may be found in Grott and Breuer (2008a).

2.2 Recent volcanism caused by mantle plumes

There are two alternative explanations for the persistence of volcanism on Mars today. Recent production of partial melt in the Martian mantle could be caused by decompression melting in the heads of uprising mantle plumes (O'Neill et al., 2007; Li and Kiefer, 2007) or by heat accumulation underneath regions of a thickened, thermally isolating crust (Schumacher and Breuer, 2007). In order to determine whether partial mantle melting is feasible on Mars today, we compare the temperature of mantle plumes to the solidus of peridotite. The effect of a thermally isolating crust will be discussed in Section 5. In our parameterized models, mantle plumes originate at the core-mantle boundary and the initial plume temperature is given by the core temperature T_c. Plumes then cool adiabatically as they rise to the surface and the plume temperature is given by

$$T_{plume} = T_c - \frac{\alpha g T_c z}{c_m} \quad (3)$$

where α is the thermal expansion coefficient, g is the gravitational acceleration, c_m is the mantle specific heat capacity and z is the distance from the core-mantle boundary.

The solidus of peridotite is determined by laboratory experiments and we use the parameterization

$$T_{sol} = 1409 + 134.2P - 6581P^2 + 0.154P^3 \quad (4)$$

where P is the pressure in GPa (Takahashi, 1990).

Given the plume and solidus temperatures T_{plume} and T_{sol}, we compute the temperature difference ΔT_{lid} between T_{plume} and T_{sol} at the base of the stagnant lid

$$\Delta T_{lid} = T_{plume,lid} - T_{sol,lid} \quad (5)$$

to determine if partial melt is generated in the convecting mantle. Furthermore, the depth of decompression melting D_{melt}, given by the depth at which T_{plume} equals T_{sol}, is also calculated to determine how deep mantle plumes would have to penetrate into the stagnant lid to generate partial melt (compare Fig. 3).

2.3 Recent volcanism caused by hydrous mantle melting

Laboratory experiments indicate that water is important for the onset of mantle melting (Hirth and Kohlstedt, 1996; Asmiov and Langmuir, 2003; Katz et al., 2003; Hirschmann, 2006) and concentrations in excess of a few hundred ppm can significantly reduce the solidus of mantle rocks. We investigate the influence of water on the solidus of peridotite using the parameterization by Katz et al. (2003). Given the bulk concentration of water in the mantle rock $X_{H_20}^{bulk}$ and the partitioning coefficient D_{H_2O} between solid and silicate melt, the concentration of water in the melt X_{H_2O} can be determined from

$$X_{H_20} = \frac{X_{H_2O}^{bulk}}{D_{H_2O} + F(1 - D_{H_2O})} \tag{6}$$

where F is the melt fraction and $D_{H_2O} = 0.01$ (Katz et al., 2003; Aubaud et al., 2004). The maximum reduction of the peridotite solidus is reached for small melt fractions and assuming $F = 0$ the maximum solidus reduction can be calculated from

$$\Delta T_{sol} = K X_{H_2O}^{\gamma} \tag{7}$$

where K and γ are experimentally determined constants and $K = 43$ °C wt%$^{-\gamma}$ and $\gamma = 0.75$ (Katz et al., 2003).

Eq. 7 is only valid for water contents X_{H_2O} smaller than the pressure dependent saturation concentration

$$X_{H_2O}^{sat} = \chi_1 P^{\lambda} + \chi_2 P \tag{8}$$

where χ_1, χ_2 and λ are experimentally determined constants and $\chi_1 = 12$ wt% GPa$^{-\lambda}$, $\chi_2 = 1$ wt% GPa^{-1} and $\lambda = 0.6$ (Katz et al., 2003). However, for the thick stagnant lids considered here, melting will occur at depths corresponding to pressures of at least 4 GPa and X_{H_2O} will always be smaller than $X_{H_2O}^{sat}$ in the models considered. Therefore, Eq. 7 will be used to estimate how much water is required to facilitate partial mantle melting.

Note that much less water is needed to be rheologically significant than what is required to appreciably lower the solidus of mantle rocks. While only 50 ppm H_2O will be 50 % saturated in olivine at 2 GPa (Hirth and Kohlstedt, 1996) and lower the viscosity by roughly one order of magnitude, 250 ppm H_2O are required to lower the peridotite solidus by 100 K (Katz et al., 2003).

3 Parameters

The simulations presented here are most sensitive to the amount and distribution of radioactive elements in the silicate portion of Mars and the efficiency of mantle energy transport. Different models for the bulk composition of Mars have been proposed (Morgan and Anders, 1979; Treiman et al., 1986; Wänke and Dreibus, 1994; Lodders and Fegley, 1997), but it seems unlikely that compositional models which generate heat at rates larger than the chondritic heat production rate (e.g., Lodders and Fegley (1997)) are representative of the planet's bulk composition (Hauck and Phillips, 2002; Grott and Breuer, 2008b). The model by Wänke and Dreibus (1994) is the one best compatible with the amount of K and Th in the near surface layers as observed by gamma ray spectroscopy (Taylor et al., 2006) and we will use this model as a reference. In the calculations, the total amount of heat producing elements ϕ will be varied between 30 and 100 % with respect to this model.

The distribution of heat producing elements between the crust and mantle is poorly constrained and crustal enrichment factors of 4 (BVSP, 1981; Nimmo and Stevenson, 2001) to 10 (Schumacher and Breuer, 2006; Grott and Breuer, 2008a; Taylor et al., 2006) with respect to the undepleted mantle are usually assumed, corresponding to a fraction of 20-50 % of heat producing elements in the crust. Because the crustal concentration factor is a function of the specific mode of crustal formation and may vary over a large range, we here assume the fraction of radioactive elements in the crust Λ to vary between 20 and 80 % (e.g., Parmentier and Zuber (2007)).

The efficiency of mantle energy transport is largely determined by the mantle viscosity, which in turn is a strong function of the mantle water content and the operating deformation mechanism. The effective viscosity $\eta = \sigma/2\dot{\epsilon}$, where σ is shear stress and $\dot{\epsilon}$ the strain rate, can be estimated from flow laws and is given by

$$\eta = \frac{\mu^n}{2A}\left(\frac{1}{\sigma}\right)^{n-1}\left(\frac{d}{b}\right)^m \exp\left(\frac{E+pV}{RT}\right) \tag{9}$$

where μ is the shear modulus, A an experimentally determined constant, d the grain size, b the Burgers vector, E the activation energy, V the activation volume, p the pressure, R the gas constant and T the temperature (Karato and Wu, 1993).

In the earth's upper mantle deformation is likely driven by non-Newtonian dislocation creep, whereas the lower activation volume of Newtonian diffusion creep favors this mechanism at greater depth, resulting in an almost depth-independent viscosity in the deep upper mantle. This transition between dislocation and diffusion creep is also supported by models of post-glacial rebound, which show that deformation is dominated by a linear rheology and allows for only a thin layer (< 200 km) of non-linearly deforming rocks (Karato and Wu, 1993). Although due to the reduced gravity the pressures in the Martian mantle are lower than those in the Earth's mantle at a given depth, it still seems likely that diffusion creep dominates the Martian mantle deformation and this will be the nominal model investigated here. However, the influence of dislocation creep will be briefly discussed in Sec. 5. We assume values of $\mu = 80$ GPa, $b = 5\cdot 10^{-10}$ m, $d = 10^{-3}$ m, $p = 3.1$ GPa and flow law parameters are adopted from Karato and Wu (1993).

The viscosity of water-saturated and anhydrous olivine varies by more than two orders of magnitude (Karato and Wu, 1993) and there is evidence that small amounts of water are present in the Martian mantle (McSween et al., 2001; Médard and Grove, 2006). Furthermore, the low elastic thickness values observed during the early Martian evolution are best compatible with a wet mantle rheology (Guest and Smrekar, 2007; Grott and Breuer, 2008a). However, to investigate the whole range of possible evolution scenarios, we will study wet as well as dry mantle rheologies.

Other parameters used in the calculations are similar to those used by Grott and Breuer (2008a) and we prescribe an initial upper mantle temperature of 1800 K, an initial core temperature of 2100 K, a crustal thermal conductivity of 3 W m^{-1} K^{-1} (Clauser and Huenges, 1995; Seipold, 1998), a mantle thermal conductivity of 4 W m^{-1} K^{-1} and a crustal thickness of 50 km (Zuber et al., 2000; Neumann et al., 2004; Wieczorek and Zuber, 2004).

The calculated elastic thickness values are sensitive to the assumed crustal and mantle rheology. Geochemical evidence suggests that the bulk of the Martian crust is basaltic (Nimmo and Tanaka, 2005) and there is ample evidence for water being abundant early in Martian history [e.g., Masson et al. (2001); Parmentier and Zuber (2007); Andrews-Hanna et al. (2007)]. Therefore, a wet diabase rheology for the Martian crust is assumed (Caristan, 1982). For the mantle, wet and dry rheologies (Karato et al., 1986) are used to be consistent with the rheology used for mantle convection.

Other parameters influencing T_e are the strain rate $\dot{\epsilon}$ and the bounding stress σ, which were chosen to be 10^{-14} s^{-1} (Phillips et al., 2008) and 10 MPa (Burov and Diament, 1995), respectively.

4 Results

4.1 Elastic thickness

Fig. 1

We have investigated the thermal evolution of Mars for a wide range of concentrations of heat producing elements and different distributions of these elements between the crust and mantle. The elastic thicknesses T_e were calculated from the lithospheric temperatures and the results of these calculations are shown in Fig. 1, where contour plots of the present day T_e are given as a function of the fraction of radiogenic elements in the crust Λ and the fraction of radiogenic elements with respect to the reference model (Wänke and Dreibus, 1994) ϕ for (a) a wet and (b) a dry mantle rheology. The shaded areas in Fig.1 correspond to models which result in elastic thicknesses in excess of 300 km.

For a wet mantle rheology (Fig.1a), the elastic thickness is larger than 300 km only if the mantle is strongly depleted of heat producing elements. This implies either a high concentration of heat producing elements in the crust of an overall low concentration in the silicate fraction. If a dry rheology is assumed (Fig. 1b), stagnant lid and elastic thicknesses increase and a higher concentration of radioactive elements in the mantle is admissible. Depending on mantle rheology, the concentration of heat producing elements in the Martian interior needs to be sub-chondritic to satisfy the constraint posed by $T_e > 300$ km. If a wet mantle rheology is assumed, the bulk concentration of radioactive elements cannot exceed 35-95 % of the reference concentration, depending on the crustal enrichment. For a dry rheology, models having 50-100 % the reference concentration of heat producing elements can satisfy $T_e > 300$ km. For a moderate crustal enrichment of 50 % (Taylor et al., 2006), the Martian bulk composition needs to be 25% and 50% sub-chondritic for wet and dry mantle rheologies, respectively.

Other parameters influencing the elastic thickness values calculated here are the assumed strain rate $\dot{\epsilon}$ and bounding stress σ_B. We have chosen a large strain rate and low bounding stress to facilitate the generation of large elastic thicknesses but a different choice of these parameters does not significantly affect the results presented here. A reduction of $\dot{\epsilon}$ by one order of magnitude decreases the elastic thickness by ∼15 km. Similarly, an increase of the bounding stress to 20 MPa decreases T_e by another ∼15 km. Fig. 2

Having identified the models which result in elastic thicknesses larger than 300 km we have investigated the elastic thickness evolution for these models as a function of time. Fig. 2 shows T_e as a function of time for (a) and (c) a wet and (b) and (d) a dry mantle rheology, varying the crustal thermal conductivity k_c. Changing the initial mantle temperature or crustal thickness has a similar influence (cp. Fig. 4 in Grott and Breuer (2008a)).

The elastic thickness estimates derived from gravity and topography data (McGovern et al., 2004; Belleguic et al., 2005; Hoogenboom and Smrekar, 2006; Wieczorek, 2008), forward modeling of thrust faults (Schultz and Watters, 2001; Grott et al., 2006), the analysis of rift flank uplift (Grott et al., 2005; Kronberg et al., 2007) and the new estimate by Phillips et al. (2008) are also shown in Fig. 2. We do not consider estimates for which only lower limits on T_e are available (Capri Chasma (McGovern et al., 2004)), as these do not serve to constrain the thermal evolution, and have substituted 0 km for a lower limit if only upper bounds existed (Hellas west rim, Hellas Basin, Noachis Terra, Northeastern Terra Cimmeria and Northeastern Arabia Terra (McGovern et al., 2004)). Also, we have calculated the mean and standard error for each structure where multiple estimates were available (Olympus, Ascraeus, Pavonis and Arsia Montes, Alba Patera and Elysium (McGovern et al., 2004; Belleguic et al., 2005)).

The time of loading for which the T_e estimates have been derived have generally only be constrained to a specific epoch, which might span several Gyr. The time coordinate of individual data-point has here been randomly assigned to fall within the corresponding epoch and the conversion to absolute ages has been achieved using the cratering chronological model of Hartmann and Neukum (2001). Timespans are 100 - 800 Myr for the Noachian, 600 - 900 Myr for the Noachian - Hesperian, 800 - 1200 Myr for the Hesperian, 900 - 2400 Myr for the Hesperian - Amazonian and 1200 - 4500 Myr for the Amazonian periods, respectively. Note that the T_e values computed using the thermal evolution model represent global averages and should not be compared to single datapoints, as individual T_e values will to some extent depend on the geological setting. Rather, they should be compared to the averages of the corresponding epochs.

For a wet mantle rheology (Fig. 2a and c) elastic thicknesses during the early evolution are satisfactorily reproduced and T_e grows rapidly after 1-1.5 Ga. Predicted elastic thicknesses during the Amazonian are larger by up to a factor of 3 than most estimates, but satisfy the constraint posed by $T_e > 300$ km today. The results are very similar if crustal concentration factors Λ of 0.5 (Fig. 2a) and 0.65 (Fig. 2c) are assumed, though larger crustal concentrations tend to yield better fits during the early evolution. The bulk concentrations of heat producing elements in Fig. 2a and c correspond to $\phi = 0.5$ and $\phi = 0.65$, respectively.

If a dry mantle rheology is assumed (Fig. 2b and d) the low elastic thickness values observed during the Noachian and early Hesperian periods are difficult to reproduce. For a moderate crustal enrichment and $\Lambda = 0.5$ elastic thicknesses rapidly grow beyond 100 km before 500 Myr. Due to the inefficient mantle cooling associated with the dry rheology, lithospheric growth is slow thereafter, but the predicted elastic thicknesses exceed most reported values in the Amazonian by up to a factor of 3. Today, T_e values of 300 km are reached.

If higher crustal enrichment factors are assumed and $\Lambda = 0.65$, the planet cools less efficiently and elastic thicknesses smaller than 50 km can be maintained up to 500 Myr. Therefore, although special parameters need to be chosen in order to fit the observations, a dry mantle rheology cannot be ruled out. The bulk concentrations of heat producing elements in Fig. 2b and d correspond to $\phi = 0.75$ and $\phi = 1$, respectively.

4.2 Recent volcanism

In order to determine whether the models resulting in $T_e > 300$ km could explain recent volcanism, we have investigated the thermal structure of the mantle and lithosphere and calculated the temperature of mantle plumes rising from the core-mantle boundary to the surface. Two representative temperature profiles for models using (a) a wet and (b) a dry mantle rheology are shown in Fig. 3. Both models result in $T_e = 300$ km today and the fraction of radiogenic elements in the crust Λ is 0.5. For the wet rheology model $\phi = 0.5$ and for the dry rheology $\phi = 0.75$, respectively. Fig. 3

Fig. 3 shows todays mantle temperature profiles calculated using the thermal evolution model, the plume temperatures calculated using Eq. 3 and the peridotite solidus. For the wet rheology (Fig. 3a), mantle energy transport is very efficient and the mantle rapidly cools, resulting in an upper mantle temperature of only 1500 K today. The plume temperature exceeds the mantle temperature by ∼40 K, but at the base of the stagnant lid the plume temperature is still ∼450 K smaller than the peridotite solidus. This implies that partial mantle melting is not expected for this model. The depth of decompression melting, given by the intersection of the plume and solidus temperatures, is ∼60 km implying that more than 85 % of the stagnant lid would need to be penetrated by the plume in order to reach this shallow depth.

If a dry rheology is assumed (Fig. 3a), mantle temperatures remain higher due to the inefficient cooling of the planet. Upper mantle temperatures are close to 1800 K and the difference between plume and solidus temperatures is ∼200 K at the base of the stagnant lid. The plume would have to rise to a depth of 280 km to initiate decompression melting, corresponding to a penetration of 35 % into the stagnant lid. Fig. 4

Fig. 4 shows the results of this analysis for the complete range of models investigated. Figs. 4a and b show contour plots of the depth of decompression melting D_{melt} with respect to the thickness of the stagnant lid D_{lid} in per cent for (a) a wet and (b) a dry mantle rheology. The temperature difference between plume temperature and the solidus of peridotite ΔT_{lid} is given in Figs. 4c and d for (c) a wet and (d) a dry mantle rheology. Shaded regions in Fig. 4 correspond to models which yield $T_e > 300$ km as determined from Fig.

1.

If a wet mantle rheology is assumed decompression melting is initiated if the plumes penetrate to depths corresponding to 15 % of the stagnant lid thickness (Figs 4a). This implies that 85 % of the lid would need to be penetrated by the plume in order to generate partial melt. For a dry mantle rheology the depth of decompression melting D_{melt} is significantly increased as the mantle temperature is large due to the inefficient mantle cooling. D_{melt} corresponds to 70 % of the stagnant lid thickness implying that only 30 % of the lid would need to be eroded by the plume (Figs 4b).

The temperature difference ΔT_{lid} between plume and solidus temperature is $\sim$400 K and $\sim$120 K for models satisfying the constraint posed by $T_e >$ 300 km for wet (Fig. 4c) and dry (Fig. 4d) mantle rheologies, respectively. As the presence of water is known to lower the peridotite solidus (Hirth and Kohlstedt, 1996; Asmiov and Langmuir, 2003; Katz et al., 2003; Hirschmann, 2006) partial mantle melting might be initiated for a wet mantle if the water concentration $X^{bulk}_{H_2O}$ is sufficiently high. Fig. 5 shows the reduction of the peridotite solidus ΔT_{sol} as a function of the water content of the mantle rocks $X^{bulk}_{H_2O}$. Given that a solidus reduction of 400 K is needed to induce partial melting, water concentrations of the order of 2000 ppm would be required. Note, however, that this may overestimate the required mantle water content as plumes might penetrate into the stagnant lid, thus reducing the difference between plume and solidus temperature ΔT_{sol}.

Fig. 5

Fig. 6

Finally we have calculated the surface heat flow F_s which can be expected if the elastic lithosphere thickness exceeds 300 km on Mars today. The results of these calculations are shown in Fig. 6, where the surface heat flow F_s is given as a function of Λ and ϕ. Depending on the crustal concentration of heat producing elements, the surface heat flow is in the range of 11-20 mW m^{-2} if a wet mantle rheology is assumed (Fig. 6a). For a dry mantle rheology, F_s is expected to be 14-20 mW m^{-2} (Fig. 6b).

5 Discussion and Conclusions

The geodynamic response of the Martian lithosphere to loading at the northern polar cap indicates that the elastic lithosphere thickness T_e is larger than 300 km at the north pole today (Phillips et al., 2008). We have reinvestigated the thermal evolution of Mars and identified models which satisfy the constraint posed by $T_e > 300$ km. Depending on the rheology of the Martian mantle, elastic lithosphere thicknesses in excess of 300 km can be obtained for sub-chondritic as well as chondritic bulk concentrations of heat producing elements. If a wet mantle rheology is assumed, the bulk concentration of radioactive elements cannot exceed 95 % of the chondritic concentration. However, for a dry mantle rheology the bulk concentration of heat producing elements does not need to be sub-chondritic, provided that heat producing elements are strongly enriched in the crust, i.e., at least 65 % of the planet's inventory of heat producing elements is situated there. For a moderate crustal enrichment of 50 % (Taylor et al., 2006), the Martian bulk composition needs to be 25% and 50% sub-chondritic for wet and dry mantle rheologies, respectively.

Having identified models satisfying $T_e > 300$ km we have compared the predicted elastic thickness evolution to the values available in the literature. Gravity and topography data (McGovern et al., 2004; Belleguic et al., 2005; Hoogenboom and Smrekar, 2006) and the analysis of rift flank uplift (Grott et al., 2005; Kronberg et al., 2007) indicate that the elastic lithosphere thickness did not exceed 40 km in the Noachian and early Hesperian periods. These low elastic thickness values are best compatible with a wet mantle rheology and a dry rheology only fits these observations if a high crustal enrichment of radiogenic elements is assumed. Therefore, although a dry mantle rheology cannot be ruled out, a wet mantle rheology is clearly preferred. These results are similar to those presented by Guest and Smrekar (2007) and Grott and Breuer (2008a), who also concluded that the low elastic thickness values in the Noachian are best compatible with wet crustal and mantle rheologies.

During the Hesperian, elastic thicknesses rapidly increase, as is also predicted by the models presented here. In our models, this increase is caused by the loss of the incompetent lower crustal layer (Guest and Smrekar, 2007; Grott and Breuer, 2008a), but a transition from a wet to a dry crustal rheology has also been considered (Guest and Smrekar, 2007).

During the Amazonian period the elastic thickness values predicted using models satisfying $T_e > 300$ km overestimate most T_e values by a factor of 2-3 and it has been speculated that this may be due to the fact that most T_e estimates in this period are associated with volcanoes and magmatic activity (Phillips et al., 2008). Thermal evolution models using chondritic concentrations of heat producing elements and $\Lambda = 50\%$ yield much better fits to the available estimates and result in elastic thicknesses of 150-200 km today (Grott and Breuer, 2008a). Therefore, it seems unlikely that large elastic thicknesses in excess of 300 km are representative for the bulk of the planet (Phillips et al., 2008).

Geological evidence suggests that Mars has been volcanically active in the recent past [e.g., Neukum et al. (2004)] and we have investigated if partial mantle melting is feasible for the models satisfying $T_e > 300$ km. We find that decompression melting in the heads of mantle plumes is possible if plumes penetrate 85 % and 30 % into the stagnant lid for wet and dry mantle rheologies, respectively. While even strong plumes are not expected to cause lithospheric undulations of the order required for a wet rheology, plumes rising 30 % into the stagnant lid can be produced if the dry mantle viscosity is strongly pressure dependent and significantly increases with depth or if endothermic phase transitions are present close to the core-mantle boundary (Buske, 2006). Therefore, decompression melting is feasible if a dry mantle rheology is assumed, but is unlikely for a wet rheology.

The temperatures underneath regions of a thickened, thermally isolating crust can locally exceed the average mantle temperature by up to 100 K (Schumacher and Breuer, 2007). Although this is surely insufficient to heat the mantle and produce partial melt for a wet mantle rheology, this effect will further reduce the depth the plumes need to penetrate if a dry mantle rheology is assumed.

If dislocation creep were the dominant deformation mechanism in the Martian mantle, energy transport would be less efficient and current mantle temperatures would be higher than those presented here. The properties of non-Newtonian rheologies can be approximated by Newtonian flow with reduced activation enthalpy (Christensen, 1984), resulting in higher average viscosities, consistent with the larger observed crustal production rates for non-Newtonian flow laws (Hauck and Phillips, 2002). Scaling laws derived from non-Newtonian mantle convection simulations (Solomatov and Moresi, 2002) indicate that time-dependent convection models using dislocation creep have mantle temperatures which are on average about 100 K higher than models using diffusion creep for similar stagnant lid thicknesses and surface heat flows. This implies that dislocation creep would make partial mantle melting easier to achieve, possibly allowing for melt production for a dry rheology without further need for strong mantle plumes.

Significant amounts of water in the Martian mantle are required to lower the mantle solidus and allow for partial mantle melting for wet mantle rheologies. While an average of 2000 ppm $X_{H_2O}^{bulk}$ is required to sufficiently lower the solidus to cause hydrous mantle melting, this amount can locally be reduced to 1300 ppm under regions of a thermally isolating crust. If dislocation creep were the dominant deformation mechanism in the Martian mantle, this could be further reduced by another 500 ppm. Although it is usually assumed that only moderate amounts of water in concentrations of 36 ppm are present in the Martian mantle (Wänke and Dreibus, 1994), no consensus on the H_2O concentration has been reached so far. Geochemical analysis of the SNC meteorites suggests that the water content of the SNC parent magmas might be as high as 1.8 wt% (McSween et al., 2001). Depending on the melt fraction, this implies a higher mantle water content (Katz et al., 2003). Trace element concentrations indicate that the melt fraction is between 2 and 10 % in the shergottites (Norman, 1999; Borg and Draper, 2003), such that locally mantle water contents of 500 to 2000 ppm H_2O seem possible. Hydrous mantle melting could therefore also account for the observed present day volcanic activity.

We conclude that although models satisfying the constraints posed by $T_e >$ 300 km and the observed recent volcanism can be constructed, special assumptions regarding the concentration and distribution of radioactive elements, the style of mantle convection and/or the mantle's volatile content need to be made. For a moderate crustal enrichment of heat producing elements the Martian bulk composition needs to be 25% and 50% sub-chondritic for wet and dry mantle rheologies, respectively. Also, if the less favored dry mantle rheology is assumed, strong plumes caused by, e.g., a strongly pressure dependent viscosity or endothermic phase transitions near the core-mantle boundary are probably required to allow for decompression melting. For a wet mantle rheology, large mantle water contents of the order of 1000 ppm are required to allow for partial mantle melting.

Even then, models resulting in a globally averaged elastic thicknesses of $T_e >$ 300 km are difficult to reconcile with most elastic thickness estimates available for the Hesperian and Amazonian periods. It therefore seems likely that elastic thicknesses in excess of 300 km are not representative for the bulk of the planet and that T_e has a large degree of spatial heterogeneity (Phillips et al., 2008).

Acknowledgments

We would like to thank R.J. Phillips and S.E. Smrekar for careful and constructive reviews, which greatly helped to improve this manuscript. This research has been supported by the Helmholtz Association through the research alliance "Planetary Evolution and Life".

References

Andrews-Hanna, J.C., R.J. Phillips, M.T. Zuber, 2007. Meridiani Planum and the global hydrology of Mars, *Nature*, 446, 163-165, doi:10.1038/nature05594.

Asimow P.D., C.H. Langmuir, 2003. The importance of water to oceanic mantle melting regimes, *Nature*, 421, 815-820, doi:10.1038/nature01429

Aubaud, C., E.H. Hauri, M.M. Hirschmann, 2004. Hydrogen partition coefficients between nominally anhydrous minerals and basaltic melts, *Geophys. Res. Lett.*, 31, 20, CiteID L20611, doi:10.1029/2004GL021341

Belleguic, V., P. Lognonne, M. Wieczorek, 2005. Constraints on the Martian lithosphere from gravity and topography data, *J. Geophys. Res.*,110, E11005, doi:10.1029/2005JE002437.

Borg, L.E., D.S. Draper, 2003. A petrogenetic model for the origin and compositional variation of the Martian basaltic meteorites, *Meteorit. Planet. Sci.*, 38, 1713-1731.

Breuer, S., T. Spohn, 2003. Early plate tectonics versus single-plate tectonics on Mars: Evidence from magnetic field history and crust evolution, *J. Geophys. Res.*, 108, E7, 8-1, 5072, doi:10.1029/2002JE001999.

BVSP (Basaltic Volcanism Study Project), Basaltic Volcanism on the Terrestrial Planets, Pergamon Press, New York, 1981.

Burov E.B., M. Diament, 1995. The effective elastic thickness (T_e) of continental lithosphere: What does it really mean?, *J. Geophys. Res.*, 100, B3, 3905-3927.

Buske, M., 2006. Three-dimensional thermal evolution models for the interior of Mars and Mercury, Ph.D Thesis, University Gttingen

Caristan, Y., 1982. The transition from high temperature creep to fracture in Maryland diabase, *J. Geophys. Res.*, 87, 6781-6790.

Christensen, U., 1984. Convection with pressure- and temperature-dependent non-Newtonian rheology, *Geophys. J. Int.*, 77, 2, 343-384, doi:10.1111/j.1365-246X.1984.tb01939.x

Clauser, C., E. Huenges, 1995. Thermal conductivity of rocks and minerals, in *Rock Physics and Phase Relations: A handbook of Physical Constants, AGU Ref. Shelf*, vol. 3, edited by T. J. Ahrens, pp. 105-126, AGU, Washington, D.C.

Grasset, O., E.M. Parmentier, 1998, Thermal convection in a volumetrically heated, infinite Prandtl number fluid with strongly temperature-dependent viscosity: Implications for planetary evolution, *J. Geophys. Res.*, 103, 18171-18181.

Grott M., 2005. Late crustal growth on Mars: Evidence from lithospheric extension, *Geophys. Res. Lett.*, 32, L23201, doi:10.1029/2005GL024492.

Grott, M., E. Hauber, S.C. Werner, P. Kronberg, G. Neukum, 2005. High Heat Flux on Ancient Mars: Evidence from Rift Flank Uplift at Coracis Fossae, *Geophys. Res. Lett.*, 32, L21201, doi:10.1029/2005GL023894

Grott, M., E. Hauber, S.C. Werner, P. Kronberg, G. Neukum, 2006. Mechanical Modeling of Thrust Faults in the Thaumasia Region, Mars, and Implications for the Noachian Heat Flux. *Icarus*, doi:10.1016/j.icarus.2006.10.001

Grott, M., D. Breuer, 2008a. The Evolution of the Martian Elastic Lithosphere and Implications for Crustal and Mantle Rheology, *Icarus*, 193, 2, 503-515, doi:10.1016/j.icarus.2007.08.015

Grott, M., D. Breuer, 2008b. Constraints on the radiogenic heat production rate in the Martian interior from viscous relaxation of crustal thickness variations, *Geophys. Res. Lett.*, 35, 5, L05201, doi:10.1029/2007GL033021

Guest, A., S.E. Smrekar, 2007. New constraints on the thermal and volatile evolution of Mars *Phys. Earth Plan. Int.*, 164, 3-4, 161-176, doi:10.1016/j.pepi.2007.06.010.

Hartmann, W.K., M. Malin, A. McEwen, M. Carr, L. Soderblom, P. Thomas, E. Danielson, P. James, J. Veverka, 1999. Evidence for recent volcanism on Mars from crater counts, *Nature*, 397, 6720, 586, doi:10.1038/17545.

Hartmann, W.K., D.C. Berman, 2000. Elysium Planitia lava flows: Crater count chronology and geological implications, *J. Geophys. Res.*, 105, E6, 15011-15026, doi:10.1029/1999JE001189.

Hartmann, W.K. and G. Neukum, 2001. Cratering Chronology and the Evolution of Mars, *Space Sci. Rev.*, 96, 165-194.

Hauck, S.A., R.J. Phillips, 2002. Thermal and crustal evolution of Mars, *J. Geophys. Res.*, 107, E7, 5052, doi:10.1029/2001JE001801.

Hirth, G., D.L. Kohlstedt, 1996. Water in the oceanic upper mantle: implications for rheology, melt extraction and the evolution of the lithosphere *Earth Plan. Sci. Lett.*, 144, 1-2, 93-108, doi:10.1016/0012-821X(96)00154-9

Hirschmann, M.M., 2006. Water, Melting, and the Deep Earth H2O Cycle *Ann. Rev. Earth Plan. Sci.*, 34, 629-653, doi:10.1146/annurev.earth.34.031405.125211

Hoogenboom, T., S.E. Smrekar, 2006. Elastic thickness estimates for the northern lowlands of Mars, *Earth Plan. Sci. Lett.*, 248, 3-4, 830-839, doi:10.1016/j.epsl.2006.06.035.

Karato, S.-I., M.S. Paterson, J.D. Fitzgerald, 1986. Rheology of synthetic olivine aggregates - Influence of grain size and water, *J. Geophys. Res.*, 91, 8151-8176.

Karato, S.-I., P. Wu, 1993. Rheology of the Upper Mantle: A Synthesis, *Science*, 260, 771-778, doi:10.1126/science.260.5109.771.

Katz, R.F., M. Spiegelman, C.H. Langmuir, 2003. A new parameterization of hydrous mantle melting, *Geochem. Geophys. Geosys.*, 4, 9, 1, CiteID 1073, doi:10.1029/2002GC000433.

Kronberg, P., E. Hauber, M. Grott, S.C. Werner, T. Schfer, K. Gwinner, B. Giese, P. Masson, G. Neukum, 2007. Acheron Fossae, Mars: Tectonic rifting, volcanism, and implications for lithospheric thickness, *J. Geophys. Res.*, 112, E04005, doi:10.1029/2006JE002780.

Li, Q., W.S. Kiefer, 2007. Mantle convection and magma production on present-day Mars: Effects of temperature-dependent rheology, *Geophys. Res. Lett.*, 34, 16, L16203, doi:10.1029/2007GL030544.

Lodders, K., B. Fegley, 1997. *Icarus*, 126, 2, 373-394, doi:10.1006/icar.1996.5653.

Masson, P., M.H. Carr, F. Costard, R. Greely, E. Hauber, R. Jaumann, 2001. Geomorphological evidence for liquid water, *Space Science Reviews*, 96, 333-364.

McGovern, P.J., S.C. Solomon, D.E. Smith, M.T. Zuber, M. Simons, M.A. Wieczorek, R.J. Phillips, G.A. Neumann, O. Aharonson, J.W. Head, 2004. Correction to "Localized gravity/topography admittance and correlation spectra on Mars: Implications for regional and global evolution", *J. Geophys.*

Res., 109, E07007.

McNutt, M.K., M. Diament, M.G. Kogan, 1988. Variations of elastic plate thickness at continental thrust belts, *J. Geophys. Res.*, 93, 8825-8838.

McSween, H.Y., T.L. Grove, R.C.F. Lentz, J.C. Dann, A.H. Holzheid, L.R. Riciputi, J.G. Ryan, 2001. Geochemical evidence for magmatic water within Mars from pyroxenes in the Shergotty meteorite, *Nature*, 409, 487-490, doi:10.1038/35054011.

Médard, E., T.L. Grove, 2006. Early hydrous melting and degassing of the Martian interior, *J. Geophys. Res.*, 111, E11, E11003, doi:10.1029/2006JE002742.

Morgan, J.W., E. Anders, 1979. Chemical composition of Mars, *Geochim. Cosmochim. Acta*, 43, 1601-1610, doi:10.1016/0016-7037(79)90180-7.

Neukum, G., R. Jaumann, H. Hoffmann, E. Hauber, J.W. Head, A.T. Basilevsky, B.A, Ivanov, S.C. Werner, S. van Gasselt, J.B. Murray, T. Mc-Cord, the HRSC Co-Investigator Team, 2004. Recent and episodic volcanic and glacial activity on Mars revealed by the High Resolution Stereo Camera, *Nature*, 432, 7020, 971-979, doi:10.1038/nature03231.

Neumann, G.A., M.T. Zuber, M.A. Wieczorek, P.J. McGovern, F.G. Lemoine and D.E. Smith, 2004. Crustal structure of Mars from gravity and topography, *J. Geophys. Res.*, 109, E08002, doi:10.1029/2004JE002262.

Nimmo, F., D.J. Stevenson, 2001. Estimates of Martian crustal thickness from viscous relaxation of topography, *J. Geophys. Res.*, 106, 5085-5098.

Nimmo, F., K. Tanaka, 2005. Early Crustal Evolution of Mars, *A.R.E.P.S.*, 33, 133-161,

Norman, M.D., 1999. The composition and thickness of the crust of Mars estimated from REE and Nd isotopic compositions of Martian meteorites, *Meteor. Planet. Sci.*, 34, 439-449.

O'Neill, C., A. Lenardic, A.M. Jellinek, W.S. Kiefer, 2007. Melt propagation and volcanism in mantle convection simulations, with applications for Martian volcanic and atmospheric evolution, *J. Geophys. Res.*, 112, E7, E07003, doi:10.1029/2006JE002799

Parmentier, E.M., M.T. Zuber, 2007. Early evolution of Mars with mantle compositional stratification or hydrothermal crustal cooling, *J. Geophys. Res.*, 112, E02007, doi:10.1029/2005JE002626.

Pettinelli, E, G. Vannaroni, A. Cereti, F. Paolucci, G. Della Monica, M. Storini, F. Bella, 2003. Frequency and time domain permittivity measurements on solid CO_2 and solid CO_2-soil mixtures as Martian soil simulants, *J. Geophyss Res.* 108, E4, 10-1, 8029, doi:10.1029/2002JE001869.

Phillips, R.J., M.T. Zuber, S.E. Smrekar, M.T. Mellon, J.W. Head, K.L Tanaka, E.N. Putzig, S.M. Milkovich, B.A. Campbell, J.J Plaut, A. Safaeinili, R. Seu, D. Biccari, L.M. Carter, G. Picardi, R. Orosei, P.S. Mohit, E. Heggy, R.W. Zurek, A.F. Egan, E. Giacomoni, F. Russo, M. Cutigni, E. Pettinelli, J.W. Holt, C.J. Leuschen, L. Marinangeli, 2008. Mars North Polar Deposits: Stratigraphy, Age, and Geodynamical Response, *Science*, 320, 5880, 1182-1185, doi:10.1126/science.1157546

Schultz, R.A., T.R. Watters, 2001. Forward mechanical modeling of the Amenthes Rupes thrust fault on Mars, *Geophys. Res. Lett.*, 28, 4659-4662.

Schumacher, S., D. Breuer, 2006. Influence of a variable thermal conductivity on the thermochemical evolution of Mars, *J. Geophys. Res.*, 111, E2, E02006, doi:10.1029/2005JE002429.

Schumacher, S., D. Breuer, 2007. An alternative mechanism for recent volcanism on Mars, *Geophys. Res. Lett.*, 34, 14, L14202, doi:10.1029/2007GL030083.

Stevenson, D.J., 2001. Mars core and magnetism, *Nature*, 412, 214-219.

Seipold, U., 1998. Temperature dependence of thermal transport properties of crystalline rocks - a general law, *Tectonophys.*, 291, 161-171, doi:10.1016/S0040-1951(98)00037-7.

Solomatov, V.S., L.-N Moresi, 2002. Scaling of time-dependent stagnant lid convection: Application to small-scale convection on Earth and other terrestrial planets, *J. Geophys. Res.*, 105, B9, 21795-21818, doi:10.1029/2000JB900197.

Takahashi, E., 1990. Speculations on the Archean mantle: Missing link between komatiite and depleted garnet peridotite, *J. Geophys. Res.*, 95, B10, 15941-15954.

Taylor, G.J., W. Boynton, J. Brckner, H. Wänke, G. Dreibus, K. Kerry, J. Keller, R. Reedy, L. Evans, R. Starr, S. Squyres, S. Karunatillake, O. Gasnault, S. Maurice, C. d'Uston, P. Englert, J. Dohm, V. Baker, D. Hamara, D. Janes, A. Sprague, K. Kim, D. Drake, 2006. Bulk composition and early differentiation of Mars, *J. Geophys. Res.*, 111, E3, E03S10, doi:10.1029/2005JE002645.

Treiman, A.H., M.J. Drake, M.-J. Janssens, R. Wolf, M. Ebihara, 1986. Core formation in the earth and shergottite parent body (SPB) - Chemical evidence from basalts, *Geochim. Cosmochim. Acta*, 50, 1071-1091, doi:10.1016/0016-7037(86)90389-3.

Wänke, H., G. Dreibus, 1994. Chemistry and accretion history of Mars, *Phil. Trans. R. Soc. London*, A, 349, 285-293.

Wieczorek, M., 2008. Constraints on the composition of the martian south polar cap from gravity and topography, *Icarus*, doi:10.1016/j.icarus.2007.10.026.

Wieczorek, M.A. and M.T. Zuber, 2004. Thickness of the Martian crust: Improved constraints from geoid-to-topography ratios, *J. Geophys. Res.*, 109, E1, E01009, doi:10.1029/2003JE002153.

Zuber M.T., S.C. Solomon, R.J. Phillips, D.E. Smith, G.L. Tyler, O. Aharonson, G. Balmino, W.B. Banerdt, J.W. Head, C.L. Johnson, F.G. Lemoine, P.J. McGovern, G.A. Neumann, D.D. Rowlands, S. Zhong, 2000. Internal Structure and Early Thermal Evolution of Mars from Mars Global Surveyor Topography and Gravity, *Science*, 287, 1788-1297.

Fig.1: Contour plots of todays elastic thickness T_e as a function of the fraction of radiogenic elements in the crust Λ and the fraction of radiogenic elements with respect to the reference model (Wänke and Dreibus, 1994) ϕ for (a) a wet and (b) a dry mantle rheology.

Fig.2: The elastic lithosphere thickness T_e as a function of time for thermal evolution models with (a) and (c) a wet and (b) and (d) a dry mantle rheology, varying the crustal thermal conductivity k_c. The bulk concentration of heat producing elements has been reduced with respect to the reference model (Wänke and Dreibus, 1994) such that todays elastic thickness is $\sim$300 km. Remaining radioactive elements have concentrations of (a) $\phi = 0.5$, (b) $\phi = 0.75$, (c) $\phi = 0.65$ and (d) $\phi = 1$ with respect to the reference model. Heat producing elements are enriched in the crust and $\Lambda = 0.5$ and 0.65 in (a)-(b) and (c)-(d), respectively. Elastic thickness estimates from the literature (see text) are also given.

Fig.3: Temperature profile in the Martian mantle and the temperature of mantle plumes as compared to the solidus temperature of peridotite for (a) a wet and (b) a dry mantle rheology. The fraction of radiogenic elements in the crust Λ is 0.5 and the fraction of radiogenic elements with respect to the reference model (Wänke and Dreibus, 1994) is (a) $\phi = 0.5$ and (b) $\phi = 0.75$, resulting in elastic thicknesses of 300 km.

Fig.4: (a)-(b): Contour plots of the depth of decompression melting in per

cent of the stagnant lid thickness as a function of the fraction of radiogenic elements in the crust Λ and the fraction of radiogenic elements with respect to the reference model (Wänke and Dreibus, 1994) ϕ for (a) a wet and (b) a dry mantle rheology. (c)-(d): Same as (a)-(b), but for the difference between the temperature at the base of the stagnant lid and the solidus temperature of peridotite. Shaded regions correspond to models resulting in $T_e > 300$ km (cp. Fig. 1).

Fig.5: Peridotite solidus reduction ΔT_{sol} as a function of water content of the mantle rock $X_{H_2O}^{bulk}$.

Fig.6: Contour plots of the surface heat flow F_s as a function of the fraction of radiogenic elements in the crust Λ and the fraction of radiogenic elements with respect to the reference model (Wänke and Dreibus, 1994) ϕ for (a) a wet and (b) a dry mantle rheology. Shaded regions correspond to models resulting in $T_e > 300$ km (cp. Fig. 1). F_s is given in mW m^{-2}.

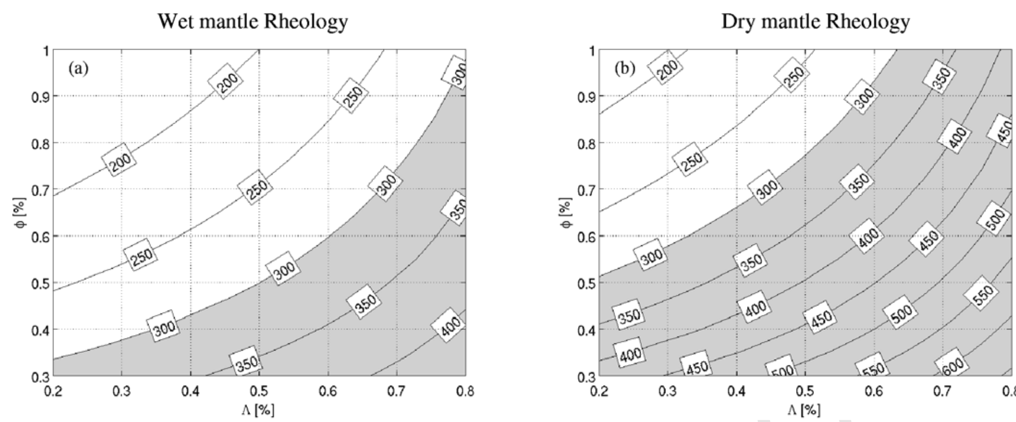
Wet mantle Rheology
Dry mantle Rheology
(a)
(b)
ϕ [%]
Λ [%]

Fig. 1.

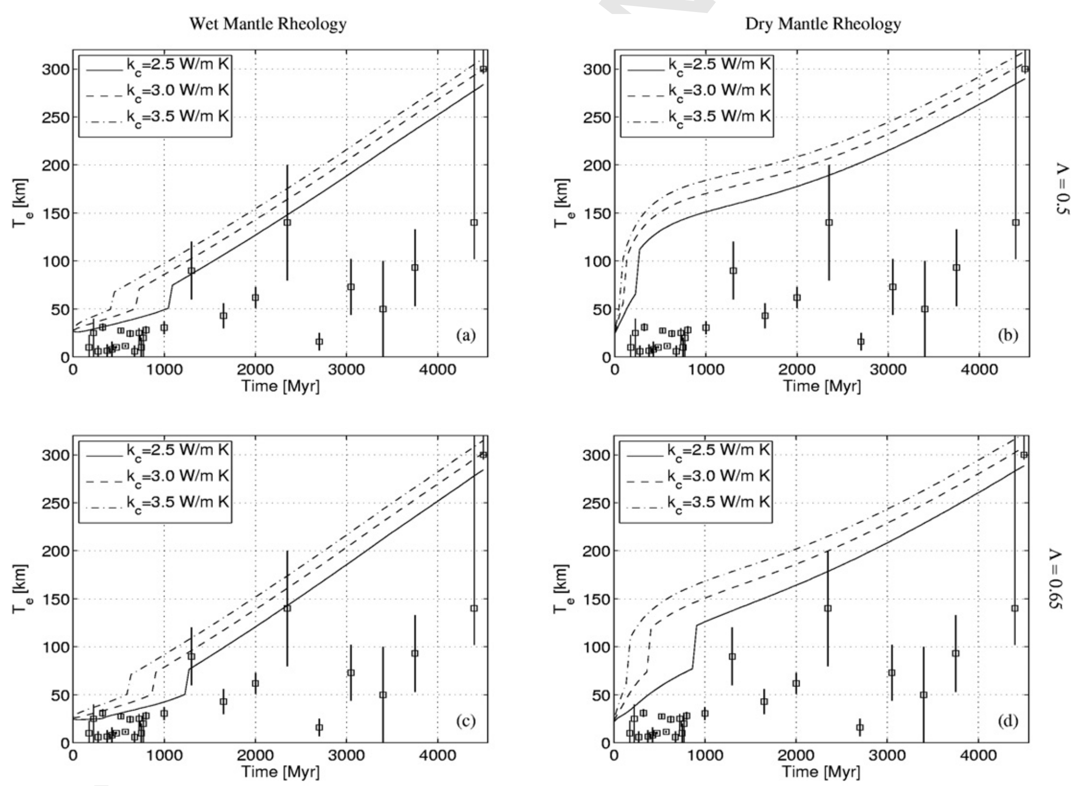
Wet Mantle Rheology
Dry Mantle Rheology
k_c=2.5 W/m K
k_c=3.0 W/m K
k_c=3.5 W/m K
T_e [km]
Time [Myr]
(a)
(b)
(c)
(d)
Λ = 0.5
Λ = 0.65

Fig. 2.

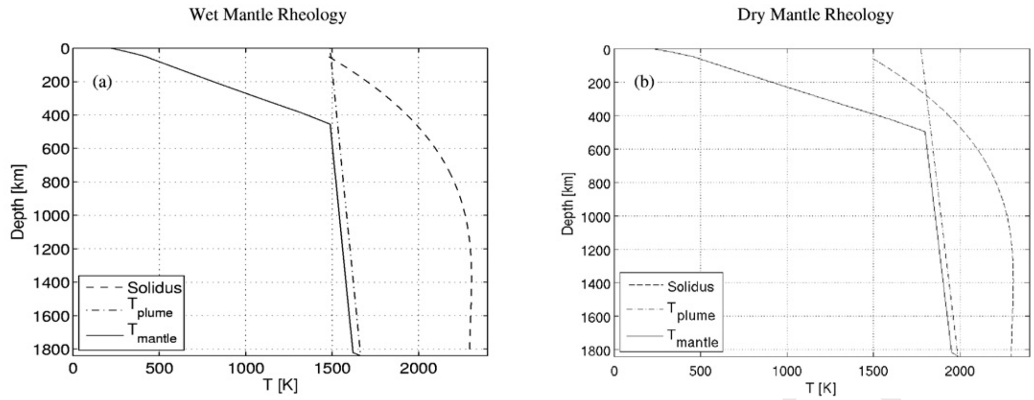

Wet Mantle Rheology
(a)
Depth [km]
T [K]
Solidus
T_{plume}
T_{mantle}
Dry Mantle Rheology
(b)

Fig. 3.

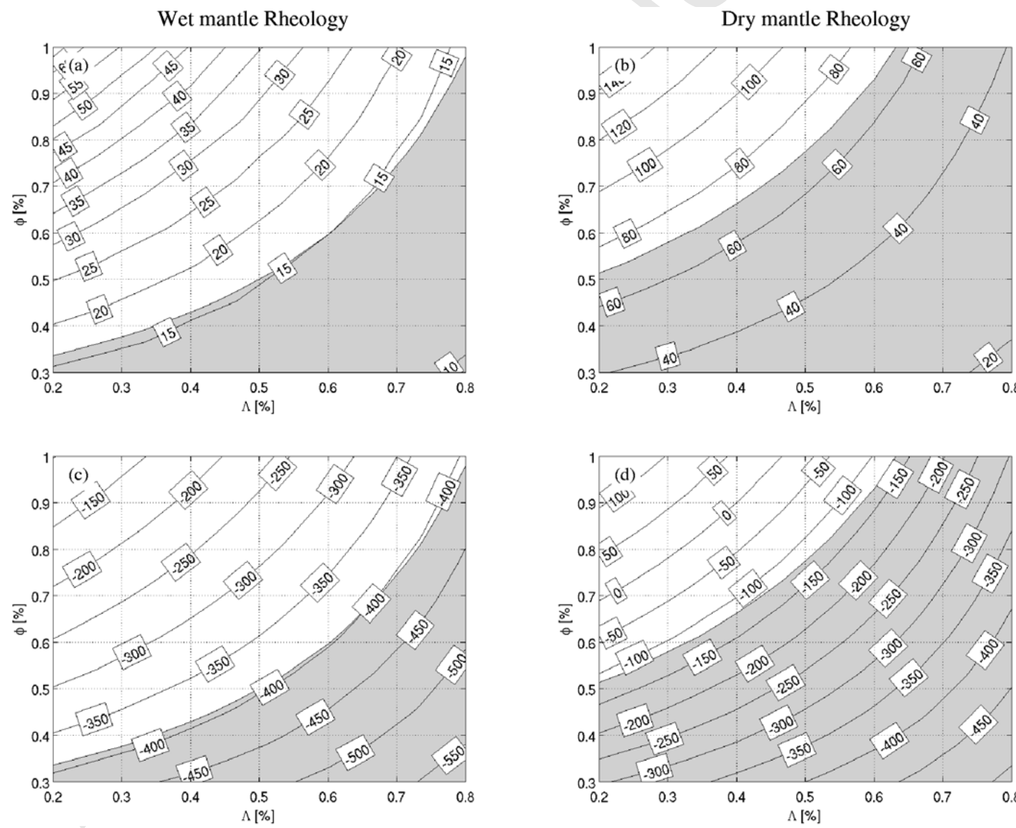

Wet mantle Rheology
Dry mantle Rheology
(a)
(b)
(c)
(d)
ϕ [%]
Λ [%]

Fig. 4.

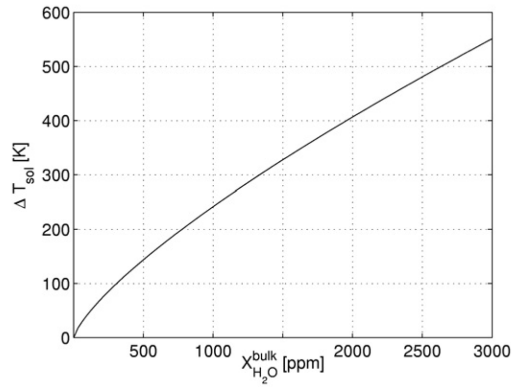

600
500
400
300
200
100
0
Δ T_sol [K]
500
1000
2000
2500
3000
X^bulk_H2O [ppm]

Fig. 5.

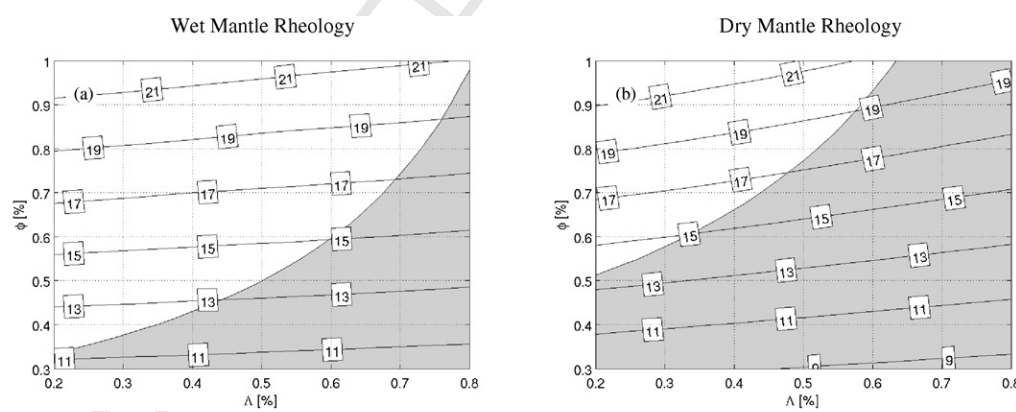

Wet Mantle Rheology
Dry Mantle Rheology
(a)
(b)
21
19
17
15
13
11
9
φ [%]
Λ [%]
0.2
0.3
0.4
0.5
0.6
0.7
0.8
0.9
1

Fig. 6.